

Internal friction of powder metallurgy (P/M) and ingot metallurgy (I/M) Al–Fe alloys at elevated temperature

T. OHASHI, Y. LIU*[‡]

*Department of Materials Science and Engineering, and *Post Graduate School, Nagoya Institute of Technology, Nagoya, Japan*
E-mail: tohashi@mse.nitech.ac.jp

Low-frequency internal friction measurements have been carried out on the powder metallurgy (P/M) and ingot metallurgy (I/M) Al–Fe alloy. Internal friction peaks can be seen at about 820–830 K and 530–620 K in the I/M alloys, but not in the P/M alloys. The former is probably due to the grain-boundary relaxation and the latter to recrystallization. Activation energies for the grain-boundary relaxation are estimated to be in two ranges: one is between 100 and 130 kJ mol⁻¹ and the other is between 200 and 210 kJ mol⁻¹, according to the iron content and fabrication processes. The high activation energy is given by the low iron content I/M alloys having a bamboo-like grain. It is suggested that such a difference in the activation energy is due to whether or not the solute iron diffuses into the grain boundary to lower the grain boundary energy. © 1998 Kluwer Academic Publishers

1. Introduction

Compared with I/M (conventional ingot metallurgy processing) aluminium alloys, P/M (powder metallurgy processing) aluminium–transition metal alloys, which are fabricated by sintering the rapidly solidified powder alloys, have excellent thermal stability and are being watched with deep interest in their application to heat-resisting materials [1, 2] because the transition metals such as iron, chromium, manganese, and so on, are commonly of low diffusivity elements in the solid aluminium compared with the other metals commercially used for alloying elements. These P/M alloys also contain a large amount of precipitates that are formed by the decomposition of the supersaturated solid solution during sintering. Such a precipitate contributes to prohibit grain-boundary sliding at high temperatures as well as to harden the alloys [3]. Grain-boundary sliding is one of the energy-dissipation processes with a relaxation time of the order of seconds [4, 5] and hence it seems helpful, in clarifying the high-temperature mechanical properties, to employ the internal friction measurements, as has been shown by the early work of Ke [6]. A typical heat-resisting P/M aluminium alloy which is often cited in the literature is Al–Fe–Ce alloy [7], and internal friction measurement was first carried out by Winholtz and Weins [8] in the temperature range from 77–700 K in order to investigate the temperature dependence of the elastic modulus for this alloy. They observed two peaks at 475 and 560 K, and thought that both peaks were associated with the grain-boundary sliding of aluminium containing precipitates. The first

peak is about 80 K lower than that of the published data on polycrystalline pure aluminium. On the other hand, many investigations of the grain-boundary relaxation in pure aluminium, where the amount of iron varies individually, have been reported [7–17], but some discrepancies in their findings can be observed, such as peak temperature, activation energy, relaxation strength, and so on. Thus, the variation in the internal friction spectrum reflecting the grain-boundary relaxation with iron content has still to be accounted for.

The aim of the present work was to reveal the effect of the precipitates and/or the solute atom of iron in aluminium on the internal friction peak and activation energy for the grain-boundary sliding by means of an internal friction technique.

2. Experimental procedure

The starting materials used in this study were high purity aluminium (99.999 mass %) and electrolytic iron (99.99 mass %). Alloy compositions of five levels, covering nominally 0.004–3 mass % Fe, were prepared. The ingots of these alloys, of dimensions 18 mm diameter and 120 mm length, were made by casting from a temperature 100 K above their liquidus temperatures to a large massive graphite mould. The melting of these alloys was achieved by using a flux for degassing and protection from oxidation. After recognizing no segregation of large intermetallic compounds by macro- and microscopic examinations of the ingots, the iron contents were analysed by X-ray fluorescence analysis

[‡] Present address: Sumitomo Light Metals Co., Nagoya, Japan.

and the results are shown in Table I. One-half of the ingots were further hot-forged and cold-drawn to wires of 1 mm diameter (I/M alloy), and the remaining ingots were subjected to melt spinning to provide liquid-quenched ribbons which were subsequently consolidated in a vacuum hot press. These consolidated alloys were then hot extruded and cold drawn to 1 mm diameter (P/M alloy). All of these cold drawn specimens were annealed for 1 h at temperatures between 673 and 873 K. Transmission electron microscopic (TEM) observations were also carried out on these wire specimens.

The internal friction, (Q^{-1}), and square of frequency were measured in a vacuum as a function of temperature by using an inverted torsion pendulum apparatus which was operated automatically by a personal computer device. The heating rate was 2 K min^{-1} for the temperature range from room temperature to 873 K. Q^{-1} was estimated from the logarithmic damping decrement $\delta = \pi Q^{-1}$.

3. Results

Grain structures of the specimens which were annealed for 1 h at 773 K changed according to the iron contents and the specimen fabrication processes. Polygonal grain structures, 90–200 μm diameter, were observed in both the P/M and I/M alloys with few exceptions; i.e. the P/M alloy of iron contents of 0.116 mass % and the I/M alloy of iron contents of 0.005 mass % are composed of elongated grains (Fig. 1a), the axial direction of which is parallel to the wire-specimens, and of a bamboo-like grain structure [13–17] (Fig. 1b), respectively. The bamboo-like grain was observed only in the I/M alloy of the lowest iron content. Changes in TEM structures according to the iron contents of the P/M alloys are also shown in Fig. 2. Apparent precipitates of Al_3Fe can be seen in the alloys of iron contents more than 0.116 mass % (Fig. 2a), and their sizes increase from tens to hundreds of nanometres with iron contents. It is pointed out that the distribution of these precipitates in the matrix grains is somewhat heterogeneous, and in the Al–3.2 mass % Fe alloy (Fig. 2b), the coarsened precipitates are at the grain boundaries as well as in the matrix grains. The grain sizes of the high iron content alloys are smaller than those of low iron content alloys, on the whole. A suitable size and distribution of the precipitates can suppress the migration of grain boundaries (Fig. 2c).

The internal friction as a function of temperature for the I/M and P/M Al–Fe alloys which were annealed for 1 h at 773 K are shown in Fig. 3a and b, respectively. Fig. 3a demonstrates that two peaks appear in each Q^{-1} spectrum of the I/M alloys, one of them in the temperature range 820–830 K and the other in the range 530–620 K. The former (high-temperature peak, *HTP*) shifts towards a higher temperature and the latter (low-temperature peak, *LTP*) does the opposite, as iron contents increase. The peak height of the LTP decreases dramatically when iron contents exceed 0.008 mass %. On the contrary, each Q^{-1} spectrum of the P/M alloys has one peak situated in the temperature range

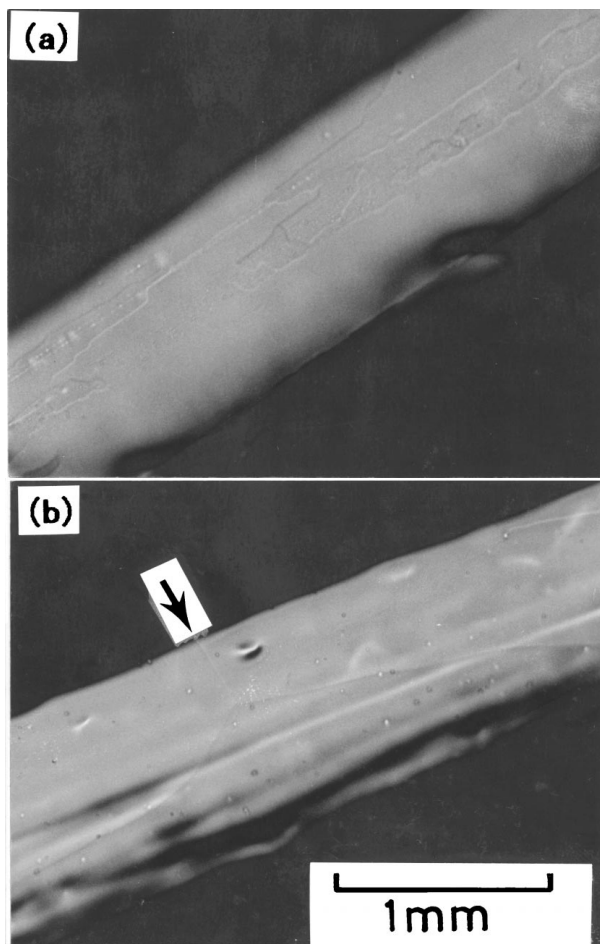


Figure 1 Photomicrographs of specimens made by P/M and I/M processes: (a) Al–0.116 mass % Fe (P/M116FE), and (b) Al–0.005 mass % Fe (P/M005FE).

500–570 K as shown in Fig. 3b. The peak temperature and peak height decrease with increasing iron contents and also, the damping capacities of the P/M alloys are lower than these of the I/M alloys as a whole. It is noteworthy that the Q^{-1} spectra of the highest iron content I/M and P/M alloys exhibit a broad and indistinct peak at about 500 K, accompanied by a high level of background damping.

Effects of annealing temperature on the peak height and peak temperature of the LTP of the I/M and P/M alloys which were surveyed in the present study are shown in Figs 4 and 5. The peak heights of the high-purity I/M alloys containing less than 0.008 mass % Fe increase remarkably with increasing annealing temperature (Fig. 4). On the other hand, all of the I/M alloys exhibit an increase in peak temperatures with annealing temperature, whereas the P/M alloys, do not; these rather decrease or do not change their peak temperatures (Fig. 5).

Fig. 6 shows the reduced values of the square of vibrational frequency $(f/f_0)^2$ which is related to the shear modulus or stiffness, plotted against temperatures for some typical I/M and P/M alloys. They decrease with increasing temperature and especially in a high-temperature range, their decrements are larger for the I/M alloys than for P/M alloys. An abrupt drop of stiffness at around 550 K is also suppressed in both the highest iron content I/M and P/M alloys, although both of

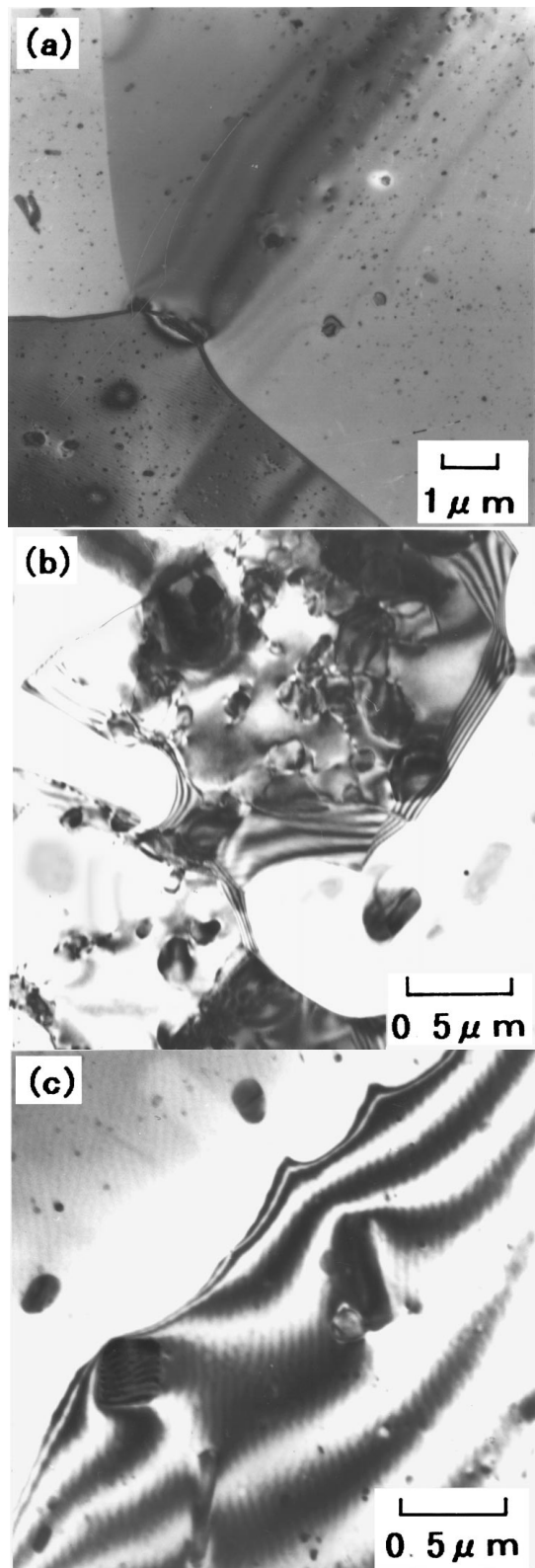


Figure 2 Change in TEM structures according to the iron content of P/M Al-Fe alloys.

the alloys result in the largest decrease in their stiffness at temperatures higher than 550 K. Here, it is pointed out that each of the highest iron content I/M and P/M alloys has a minimum in the curve of $(f/f_0)^2$ versus temperature at around 820–830 K which exactly correspond to the temperatures of HTP in Q^{-1} spectra, as mentioned above. Such a minimum or HTP could be detected during heating up to 873 K but not during

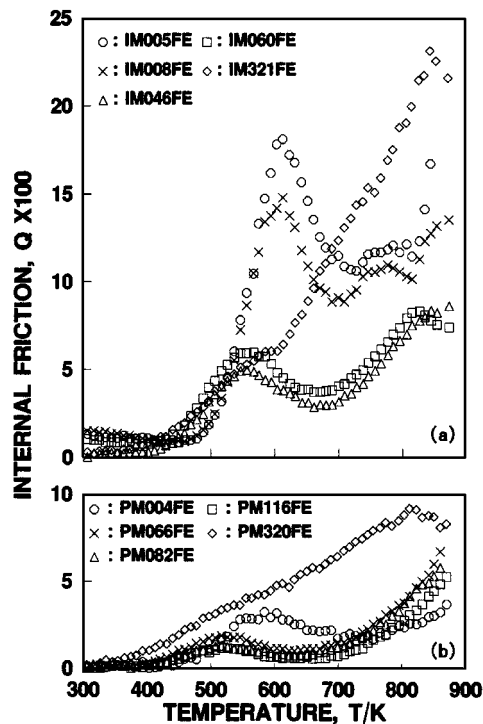


Figure 3 Internal friction as a function of temperature for the (a) I/M and (b) P/M Al-Fe alloys which were annealed for 1 h at 773 K. (a) (○) IM005FE, (×) IM008FE, (△) IM046FE, (□) IM060FE, (◇) IM321FE. (b) (○) PM004FE, (×) PM066FE, (△) PM082FE, (□) PM116FE, (◇) PM320FE.

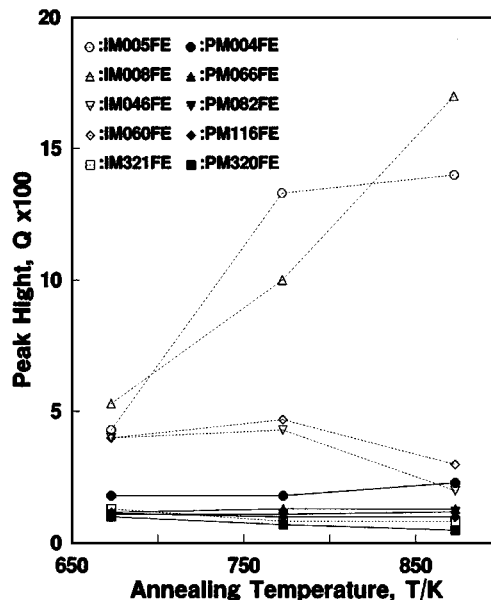


Figure 4 Effect of annealing temperature on the peak height of the I/M and P/M Al-Fe alloys. (○) IM005FE, (△) IM008FE, (▽) IM046FE, (◇) IM060FE, (□) IM321FE, (●) PM004FE, (▲) PM066FE, (▼) PM082FE, (◆) PM116FE, (■) PM320FE.

cooling to room temperature and hence its behaviour is irreversible. Temperatures giving such a minimum accompanying HTP were also lowered by lowering the annealing temperatures and the same was true for the other low iron content alloys. It can be concluded from such irreversible behaviour that the appearance of $(f/f_0)^2$ minimum and/or HTP should be caused by recrystallization of the aluminium grains. On the contrary, the

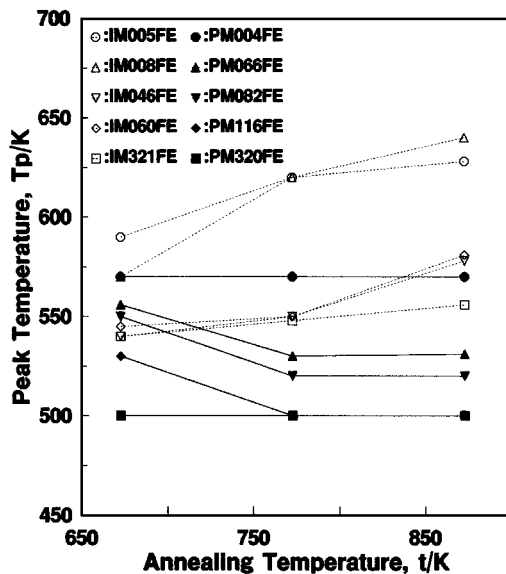


Figure 5 Effect of annealing temperature on the peak temperature of the I/M and P/M Al-Fe alloys. For key, see Fig. 4.

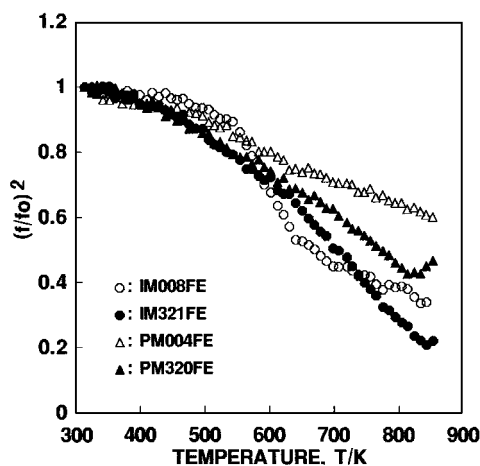


Figure 6 Reduced values of the square of vibrational frequency $(f/f_0)^2$ against temperatures for some typical I/M and P/M Al-Fe alloys. (○) IM008FE, (●) IM321FE, (△) PM004FE, (▲) PM320FE.

behaviour of LTP is reversible for temperature, and well associated with the grain-boundary sliding.

Here, it is convenient to characterize a damping process by the so-called relaxation strength, Δ , which is related to the logarithmic decrement δ or $\delta/\pi = Q^{-1}$ by the relationship [4]

$$\delta/\pi = \Delta \omega \tau / (1 + \omega^2 \tau^2) \quad (1)$$

where ω and τ are the circular frequency of vibration and the relaxation time at constant stress, respectively. Equation 1 is the so-called the Debye equation and corresponds to a single relaxation time. The observed Q^{-1} spectra, which are normalized by the each maximum Q_m^{-1} , are shown in Fig. 7a and b as a function of $\ln(\omega\tau)$. These spectra are wider than that expected for Equation 1 and suggest that the damping process has a wide range of relaxation times. Thus, a log normal distribution in τ has been introduced into the theoretical internal friction equations by Nowick and Berry ([4] p. 94). The parameter β appearing in its distribution

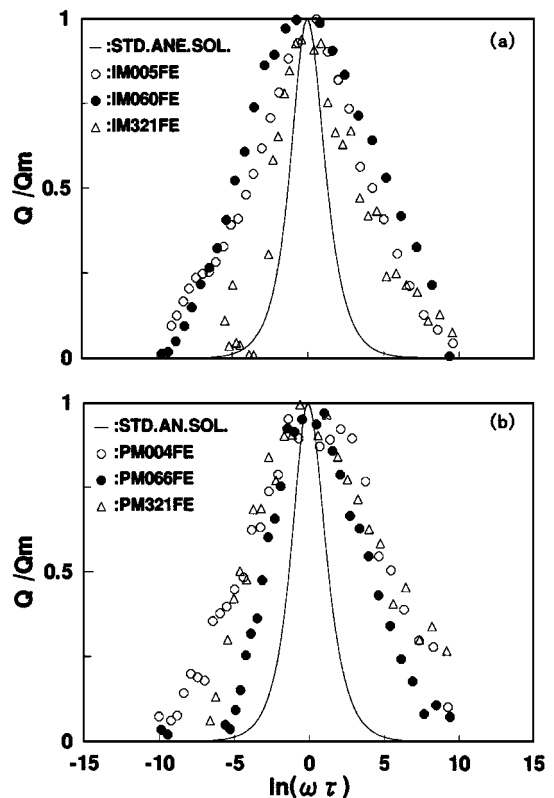


Figure 7 Normalized Q^{-1} spectra of the (a) I/M and (b) P/M alloys as a function of $\ln(\omega\tau)$. (—) Std. Ane. Sol. (a) (○) IM005FE, (●) IM060FE, (△) IM321FE. (b) (○) PM004FE, (●) PM066FE, (△) PM321FE.

function is expressed by the half-width of the distribution in τ when the value of the distribution function is $1/e$ of its maximum. When the distribution of τ obeys a Debye peak, $\beta = 0$. The values of β and Δ can be estimated from the dependence of the relative peak height and the relative peak width on the distribution parameter β , and they are tabulated in Table I. As can be seen, β values are in a range between 1 and 3.6, suggesting that the relaxation does not proceed in a single manner.

It can be assumed that the relaxation rate, τ^{-1} , is expressed by an Arrhenius equation; then Q^{-1} gives rise to a peak located at temperature T_p which is defined by

$$\omega \tau_0 \exp(Q_f/RT_p) = 1 \quad (2)$$

where Q_f is the activation energy for the damping process, R the gas constant, T_p the absolute temperature at which the peak of the Q^{-1} spectrum is observed for a fixed frequency, ω , and τ_0 is a frequency factor. When the frequency is changed, the activation energy, Q_f , can be estimated by the $\ln \omega$ versus $1/T_p$ relationship. An example of the Q^{-1} peak shift in the normalized Q^{-1} spectra is shown in Fig. 8 for a specimen of PM082FE. The activation energies, Q_f , obtained by this method are also tabulated in Table I.

4. Discussion

As shown in Table I, the activation energy of grain-boundary relaxation varies from a level of 100–130 kJ

TABLE I Grain-boundary relaxation parameters of Al-Fe alloys

Processing	Fe content (mass %)	Activation energy (kJ mol ⁻¹)	Distribution parameter, β	Relaxation strength, Δ	τ_m (s)
P/M	0.004	205	3.6	0.11	8.0×10^{-2}
	0.066	120	1.7	0.05	8.0×10^{-2}
	0.082	130	1.5	0.03	8.0×10^{-2}
	3.200	133	2.8	0.05	8.0×10^{-2}
I/M	0.005 ^a	210	1.7	0.48	2.0×10^{-2}
	0.060	200	3.1	0.02	8.0×10^{-2}
	3.210	102	1.0	0.04	8.0×10^{-2}

^aBamboo structure.

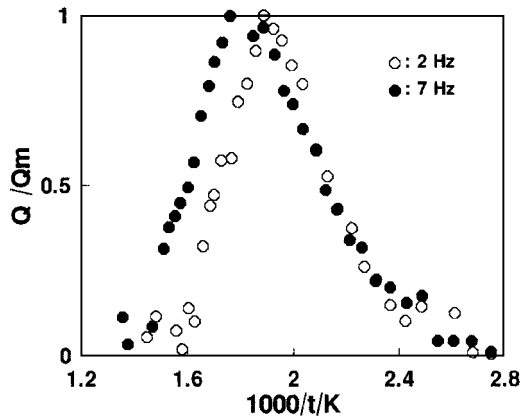


Figure 8 Example of Q^{-1} peak shift in the normalized spectra for the specimen of PM082FE. (○) 2 Hz, (●) 7 Hz.

mol⁻¹ to that of 200–210 kJ mol⁻¹ according to the iron content and fabrication process. The activation energy, Q_f , of 200–210 kJ mol⁻¹ level is rather given by low iron content alloys such as IM005FE (bamboo grain structure), IM060FE and PM004FE. Such a high activation energy has been also given in the grain-boundary relaxation of the bamboo structure [13] and is higher than that for the self-diffusion of aluminium in its bulk, which is in the range of 126–144 kJ mol⁻¹ [18]. The activation energy, Q_d , for the diffusion of the solute iron in aluminium is estimated to be 180–190 kJ mol⁻¹ according to Brandes and Brook [18] of tracer impurity diffusion tests on 99.995% and 99.999% aluminium. These values are more or less well in agreement with the high activation energies for the large or bamboo-like grain-boundary relaxation as shown in the present work. Therefore, it is suggested that if the aluminium contains a greater or lesser amount of iron, the grain-boundary relaxation of the large grain structures, including the bamboo grain structure, is controlled by iron bulk diffusion.

After Ashby [19], a high-angle grain-boundary sliding should be accompanied by migration of the boundary to avoid any change of the boundary structure and energy. According to the Gibbs' adsorption Equation [2], the interface energy is lowered by the segregation of solute into the interface such as a grain boundary. Hence, if solute atoms segregate at the grain boundaries, the grain-boundary sliding accompanied by their migration makes the boundary draw away from its segregated solute atmosphere and the solute must diffuse to keep up with the boundary by bulk diffusion, which

causes the activation energy for the grain-boundary diffusion to switch to that for the bulk diffusion of solute. When the iron content exceeds the solubility limit which is in 0.03–0.05 mass % at the eutectic reaction temperature of 928 K [21], Q_f decreases abruptly to a level of 100–130 kJ mol⁻¹ which is almost in the range of the activation energy for the self-diffusion of aluminium (126–144 kJ mol⁻¹ [18]). The excess solute iron has to precipitate and forms the intermetallic compound of Al₃Fe in order to keep the thermodynamic equilibrium at the grain boundaries, and then the solute iron content increases to its saturated concentration. Attaining such a situation results in the reduction of the diffusion of the solute iron into the grain boundaries and also in the restriction of the grain-boundary migration by the pinning effect of Al₃Fe. Thus, the bulk diffusion of aluminium will be practically important to avoid any change of the boundary structure and energy during grain-boundary sliding. This idea leads us to imply that Q_f and T_p , each of which is mutually connected by Equation 2, decrease with increasing iron content.

Now, it can be seen that there is an iron content which brings about an abrupt decrease in Q_f (see Q_f values of P/M066FE and I/M060FE in Table I) and its content is a somewhat noteworthy difference between the I/M and P/M alloys. Such an iron content is less in P/M alloy than in I/M alloy. This might be due to the oxide particles of Al₂O₃ distributed in the P/M alloys, i.e. when the melt-spun ribbons are consolidated by hot pressing and extrusion, the Al₂O₃ layer on the surface of the ribbons is brokening to pieces. These Al₂O₃ particles pin the grain boundaries, so that the grain-boundary migration is restricted and the diffusion of iron towards the grain boundaries is no longer required. Thus, the activation energy, Q_f , approaches that for the self-diffusion of aluminium.

According to the model of the grain-boundary sliding based on its viscous behaviour [4], the relaxation strength, Δ , can be linearly related to the sliding distance of the grain boundary which is controlled by the triple grain junctions, grain-boundary dislocations, leges, and pinning particles [19]. Thus, when the number of the triple grain junctions decreases with an increase in the grain size, the resultant sliding distance can produce a large relaxation strength, Δ . Hence, it can be seen in Figs 3 and 4, or Table I, that the annealed alloys such as IM005FE and IM008FE containing the least amount of iron and having large or bamboo-like grains, give a large Δ .

Acknowledgement

The authors thank the Light Metals Educational Foundation Inc. (Osaka, Japan) for financial support.

References

1. G. LUTJERING, B. SOPART and J. ALBRECHT, in "Proceedings of the International Conference RASELM" (Japanese Institute of Light Metals) p. 27.
2. F. H. FRORES, C. SURYANARANARA and E. LVERNIA, *ibid.*, p. 43.
3. D. ALTENPOHL, in "Aluminium und Aliminium Legierungen" (Springer, 1965) p. 698.
4. A. S. NOWICK and B. S. BERRY, in "Anelastic Relaxation in Crystalline Solids" (Academic Press, 1972) p. 435.
5. H. G. GLEITER and B. CHALMERS, *Progr. Mater. Sci.* Vol **16** (1972) 219.
6. T. S. KÊ, *Phys. Rev.* **72** (1947) 41.
7. W. M. GRIFFTH, R. E. SANDERS JR and G. J. HILDEMAN, in "High-Strength Powder Metallurgy Aluminum Alloys" (The Metallurgical Society of AIME, 1982) p. 209.
8. R. A. WINHOLTZ and W. N. WEINS, *J. Physique* **46** (1985) C10-375.
9. J. N. CORDEA and J. W. SPRENTNAK, *Trans. Metall. Soc. AIME* **236** (1966) 1685.
10. E. A. ATTIA, *Br. J. Appl. Phys.* **18** (1967) 1343.
11. A. A. GALKIN, O. I. DATSKO, V. I. ZAYTSEV and G. A. MATININ, *Phys. Met. Metallog.* **28** (1969) 207.
12. B. YA. PINES and A. A. KARMAZIN, *ibid.* **29** (1970) 197.
13. Y. OGINO and Y. AMANO, *Trans. JIM* **20** (1979) 81.
14. K. KAWASAKI, *Phys. Status Solidi (a)* **79** (1983) 115.
15. P. CUI, Q. HUANG T. S. KÊ and S. C. YAN, *ibid.* **86** (1984) 593.
16. B. L. CHEN and T. S. KÊ, *ibid.* **107** (1988) 177.
17. T. S. KÊ and A. W. ZHU, *Phys. Status Solidi (a)* **113** (1989) k195.
18. E. A. BRANDES and G. B. BROOK, in "Smithells Metals Reference Book," 7th Ed (Butterworth-Heinemann, 1992) p. 13-9.
19. M. F. ASHBY, *Surf. Sci.* **31** (1972) 498.
20. R. A. SWALIN, in "Thermodynamics of solids" (Wiley, 1972) p. 220.
21. L. F. MONDOLFO, in "Aluminum Alloys: structure and properties" (Butterworth, 1976) p. 282.

Received 15 December 1997
and accepted 5 August 1998